AT&T Technical Journal
Vol. 64, No. 8, October 1985
Printed in U.S.A.

# Baseband Cross-Polarization Interference Cancellation for M-Quadrature Amplitude-Modulated Signals Over Multipath Fading Radio Channels

By M. KAVEHRAD*

(Manuscript received March 21, 1985)

In this paper we propose a novel baseband structure capable of adaptively mitigating cross-polarization interference in a dual-polarized, M-state quadrature amplitude-modulated received signal. We show that by using this canceler, performance signatures very close to single-polarized system signatures can be achieved for dually polarized digital radio systems.

## I. INTRODUCTION

Because of frequency reuse via orthogonally polarized channels, dual-polarized transmission of M-state Quadrature Amplitude-Modulated (M-QAM) signals can double the bandwidth efficiency of terrestrial radio routes. Such systems transmit two different information signals of the same bandwidth and the same carrier frequency by using orthogonal field polarization for the transmission of each signal. Nonideal antennas and transmission media cause cross-coupling of the two signals and cross-polarization interference. Cross-polarization interference cancellation using adaptive transversal filters over linear dispersive multipath channels has been the subject of considerable prior investigation.[1-4]

In this study we deal with cross-polarization interference cancella-

* AT&T Bell Laboratories.

tion and intersymbol interferance (ISI) equalization separately, and propose a novel method of cross-polarization cancellation for dual-polarized operation of M-QAM signals over dispersive fading channels, similar to those experienced in line-of-sight terrestrial radio applications. The canceler operates at baseband and improves the dual-polarized system performance to very nearly the performance of a single-polarized system.

The canceler design is based on a previous observation that the power loss associated with a cross-coupled signal subject to flat or mildly dispersive fading brings about an actual reduction in system outage time.[5] In this paper we use the model and results of Ref. 5 to introduce the canceler structure and evaluate its performance. To enable comparison in the absence of cancellation, we use a dual-polarized system performance signature (M-curve) as a measure in our evaluation.[5]

In the following section we review the results of Ref. 5 briefly, and then introduce discussions leading to the realization of the canceler. In Section III the canceler performance for both dual-polarized 16- and 64-QAM radio systems is presented and the results are discussed in detail.

## II. ANALYTICAL MODEL

In this section we describe briefly the channel model and underlying assumptions germane to baseband cancellation, and then introduce the canceler model.

### *2.1 Channel model*

The dual-polarized channel model is shown in Fig. 1. Two inde-

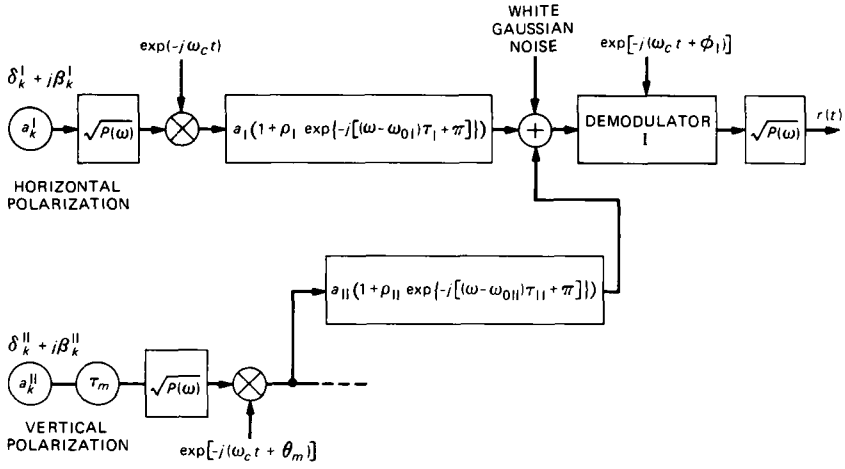


Fig. 1—Channel model for a dual-polarized system.

pendent data streams are separately modulated and transmitted cochannel, using orthogonal polarizations. Rummler's multipath fading model, which assumes the presence of a single inband notch, is applied to both the copolarized and the cross-coupled interfering channel transfer functions.[6] In other words, fadings of both the desired copolarized and cross-polarized interference channels are assumed to be the single notch type and independent. As depicted in Fig. 1 and derived in detail in Ref. 5, the received in-phase signal on the reference copolarized path is denoted by $r_{i,\mathrm{I}}(t)$;

$$
\begin{aligned}
r_{i,\mathrm{I}}(t) = {} & a_{\mathrm{I}}\delta_0^{\mathrm{I}}\{\cos(\phi_{\mathrm{I}})p(t) + \rho_{\mathrm{I}}\cos[(\omega_c - \omega_{0\mathrm{I}})\tau_{\mathrm{I}} + \pi + \phi_{\mathrm{I}}]p(t - \tau_{\mathrm{I}})\} \\
& + a_{\mathrm{I}} \sum_{k\neq 0} \delta_k^{\mathrm{I}}\{\cos(\phi_{\mathrm{I}})p(t - kT_s) + \rho_{\mathrm{I}}\cos[(\omega_c - \omega_{0\mathrm{I}})\tau_{\mathrm{I}} + \pi + \phi_{\mathrm{I}}] \\
& \quad \cdot p(t - kT_s - \tau_{\mathrm{I}})\} \\
& + a_{\mathrm{I}} \sum_{k} \beta_k^{\mathrm{I}}\{\sin(\phi_{\mathrm{I}})p(t - kT_s) + \rho_{\mathrm{I}}\sin[(\omega_c - \omega_{0\mathrm{I}})\tau_{\mathrm{I}} + \pi + \phi_{\mathrm{I}}] \\
& \quad \cdot p(t - kT_s - \tau_{\mathrm{I}})\} \\
& + a_{\mathrm{II}} \sum_{k} \delta_k^{\mathrm{II}}\{\cos(\phi_{\mathrm{I}} + \theta_m)p(t - kT_s - \tau_m) \\
& + \rho_{\mathrm{II}}\cos[(\omega_c - \omega_{0\mathrm{II}})\tau_{\mathrm{II}} + \pi + \phi_{\mathrm{I}} + \theta_m]p(t - kT_s - \tau_{\mathrm{II}} - \tau_m)\} \\
& + a_{\mathrm{II}} \sum_{k} \beta_k^{\mathrm{II}}\{\sin(\phi_{\mathrm{I}} + \theta_m)p(t - kT_s - \tau_m) \\
& + \rho_{\mathrm{II}}\sin[(\omega_c - \omega_{0\mathrm{II}})\tau_{\mathrm{II}} + \pi + \phi_{\mathrm{I}} + \theta_m]p(t - kT_s - \tau_{\mathrm{II}} - \tau_m)\} \\
& + \mathrm{Re}\{n_{\mathrm{I}}(t)\}, \qquad (1)
\end{aligned}
$$

where $\mathrm{Re}\{\cdot\}$ stands for real part. In this equation, $(\delta_k^i, \beta_k^i)$ $i = \mathrm{I}, \mathrm{II}$ represent the real and imaginary parts of the complex-valued transmitted symbols on the two polarizations, I and II, at consecutive instants, $kT_s$, $k = 0, 1, 2, \cdots$, where $T_s$ is a baud period. The Nyquist-shaping filter impulse response is denoted by $p(t)$, and $\omega_c$ is the nominal carrier frequency. The parameters $a_i$, $\rho_i$, $\omega_{0i}$, $\tau_i$; $i = \mathrm{I}, \mathrm{II}$ represent the flat fade level, fade notch depth, fade notch position, and relative delay between the two rays in each of the Rummler type multipath fading models (the reference copolarized and the corresponding cross-coupled interfering channels). Also, in eq. (1), $\tau_m$ and $\theta_m$ account for any symbol timing or carrier phase asynchronism that may exist between the two polarized signals at the transmitter location.

It might be worthwhile, at this point, to discuss the impact of transmitter local oscillators status on the theoretical modeling of the channel. Illustrated in Fig. 2 is a typical dual-polarized system transmitter configuration. As seen, there are three major sets of local oscillators in the transmitter system that can play an important role

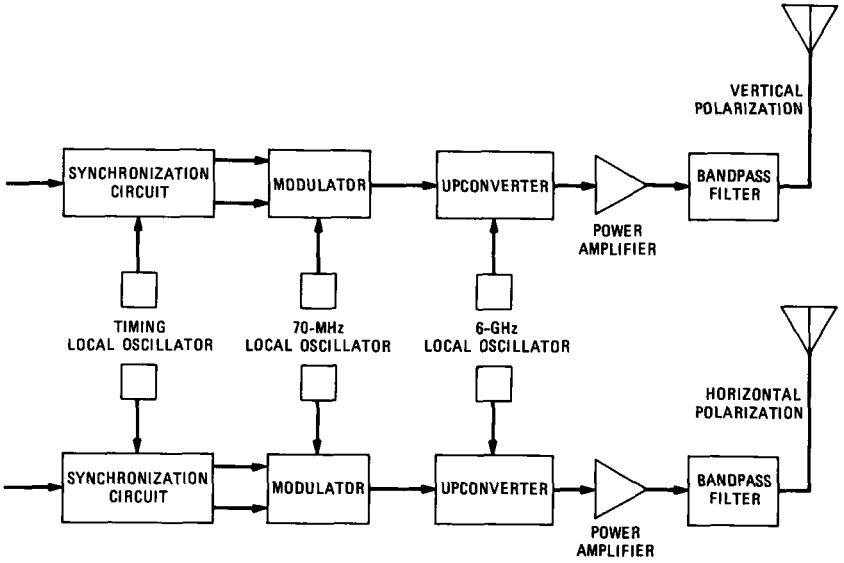


Fig. 2—A dual-polarized system transmitter.

in modeling a dual-polarized system. Namely, local oscillators used to provide clock timing to baseband sequences, IF local oscillators providing carrier signals to modulators, and microwave upconverter oscillators. Because we intend to introduce baseband cancellation in the following sections, receiver implementation is simpler if we synchronize all the transmitter local oscillators. In other words, we assume $\tau_m = 0$ and $\theta_m = 0$ and investigate the overall system performance. This assumption also results in improved performance of the cross-polarization interference canceler as was demonstrated in Ref. 5 for the general dual-polarized system performance signatures in the absence of a canceler.

The optimum phase between the modulator and the demodulator of the reference copolarized signal ($i = \mathrm{I}$) for optimum timing is introduced by $\phi_{\mathrm{I}}$. Note that for a strong main polarization signal and because of the independence assumption on the cross-coupled signal, $\phi_{\mathrm{I}}$ is imposed on the latter by the copolarized signal demodulator.[5]

As noted in eq. (1), the dispersive nature of the multipath channel is completely described by the superposition of four impulse responses, each weighted by an appropriate independent transmitted symbol state. These impulse responses for the $k$th transmitted symbol intervals are

$$u_{i,\mathrm{I}} = a_{\mathrm{I}}\{p(t - kT_s)\cos(\phi_{\mathrm{I}}) + \rho_{\mathrm{I}}p(t - kT_s - \tau_{\mathrm{I}})\cos[(\omega_c - \omega_{0\mathrm{I}})\tau_{\mathrm{I}} + \pi + \phi_{\mathrm{I}}]\}, \quad (2a)$$

$$u_{q,\mathrm{I}} = a_{\mathrm{I}}\{p(t - kT_s)\sin(\phi_{\mathrm{I}}) + \rho_{\mathrm{I}}p(t - kT_s - \tau_{\mathrm{I}})\sin[(\omega_c - \omega_{0\mathrm{I}})\tau_{\mathrm{I}} + \pi + \phi_{\mathrm{I}}]\}, \quad (2b)$$

$$u_{i,\mathrm{II}} = a_{\mathrm{II}}\{p(t - kT_s - \tau_m)\cos(\phi_{\mathrm{I}} + \theta_m) + \rho_{\mathrm{II}}p(t - kT_s - \tau_{\mathrm{II}} - \tau_m) \cdot\cos[(\omega_c - \omega_{0\mathrm{II}})\tau_{\mathrm{II}} + \pi + \phi_{\mathrm{I}} + \theta_m]\}, \quad (2c)$$

and

$$u_{q,\mathrm{II}} = a_{\mathrm{II}}\{p(t - kT_s - \tau_m)\sin(\phi_{\mathrm{I}} + \theta_m) + \rho_{\mathrm{II}}p(t - kT_s - \tau_{\mathrm{II}} - \tau_m)\sin[(\omega_c - \omega_{0\mathrm{II}})\tau_{\mathrm{II}} + \pi + \phi_{\mathrm{I}} + \theta_m]\}, \quad (2d)$$

where the variables have been previously defined. For the received in-phase part of the main polarization signal, eqs. (2a) and (2b) describe the distorted in-phase and quadrature-coupled signals of the reference copolarized transmitter, respectively, and equations (2c) and (2d) describe the corresponding signals from the cross-polarized interferer.

To introduce the parameters that define the fading character of the interfering cross-coupled signal path, we associated with each interferer fading event a triplet representing its dispersive fading status. This triplet is

$$\left[20 \log \frac{a_{\mathrm{II}}}{a_{\mathrm{I}}}\,(\mathrm{dB}),\ -20 \log |1 - \rho_{\mathrm{II}}|\,(\mathrm{dB}),\ \Delta f_{0\mathrm{II}}(\mathrm{MHz})\right], \quad (3)$$

where $a_{\mathrm{II}}$ and $a_{\mathrm{I}}$ represent the flat fade levels for cross-coupled and copolarized signals, respectively. In the triplet, the second term is dispersive fade notch depth, and $\Delta f_{0\mathrm{II}}$ denotes fade notch position relative to the carrier frequency of the cross-coupled channel. (Notice that other definitions of notch depth can be found in the literature.[4]) For illustrative purposes, we demonstrate eqs. (2a) through (2d) in Figs. 3 and 4, an interferer of (−20, 0, 0) fade and two different fade conditions of the reference main polarization path (copolarized channel). In Fig. 3 we illustrate the aforementioned impulse responses when a notch-centered fade of 10 dB is applied to the main polarization signal. Observe that since the fade on the latter is notch centered and $\theta_m = 0$, $u_{q,\mathrm{I}}$ and $u_{q,\mathrm{II}}$ are both zero. In Fig. 4 an 11-MHz offset fade of 7.5 dB is applied to the main polarization path, and even though the interferer has a flat fade, because of the phase $\phi_{\mathrm{I}}$ imposed on it, $u_{i,\mathrm{II}}$ and $u_{q,\mathrm{II}}$ are nonzero Nyquist-shaped pulses with their relative positions also determined by the phase and timing imposed on them by the dominant polarization signal.

Now we define a decision variable which is a function of the desired symbol to be detected, intersymbol interference, cross-polarized interference, and Gaussian noise. To evaluate the average error probability, first we derive the conditional error probability conditioned on the

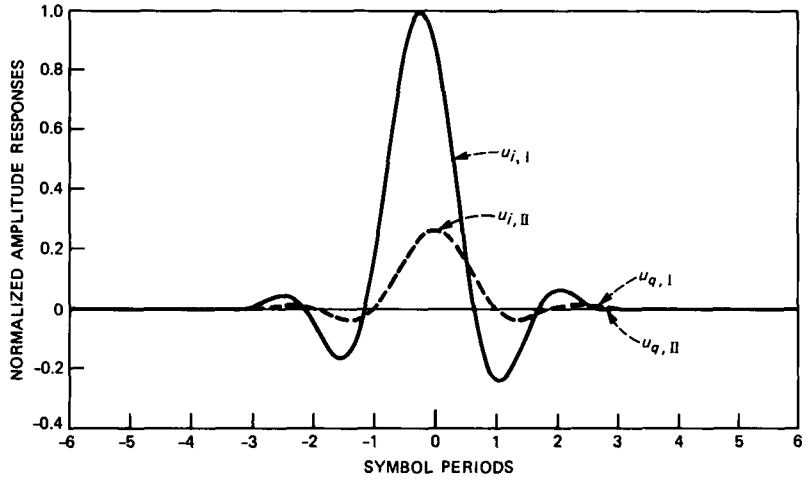


Fig. 3—16-QAM signal, time-domain impulse responses for a notch-centered fade.

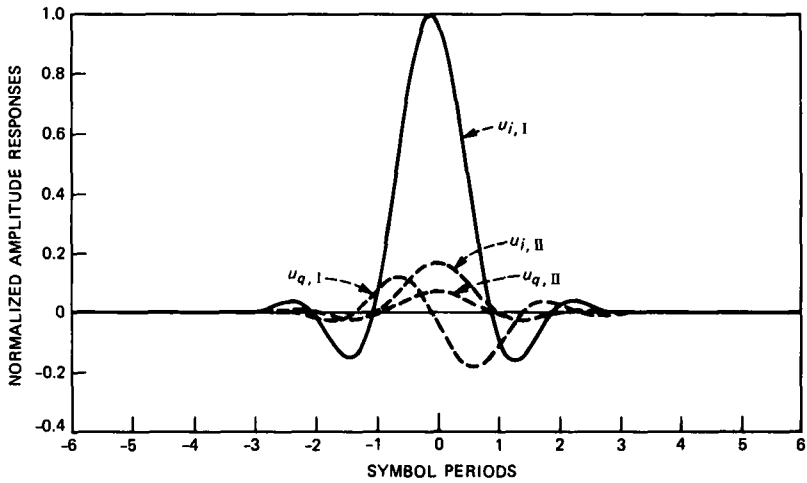


Fig. 4—16-QAM signal, time-domain impulse responses for an offset fade.

composite interference. Then by applying moment-generating functions and the Gauss quadrature method, we determine the average error probability. The details of this procedure are explained in Ref. 5.

Using eq. (1), we then computed the performance signatures (M-curves) of the main (reference) polarization signal ($i$ = I) that provide a locus of the fade notch depth (in dB) versus the relative fade notch position (in MHz) for a $10^{-3}$ average probability of error. In Fig. 5 we illustrate the performance signatures of the main polarization

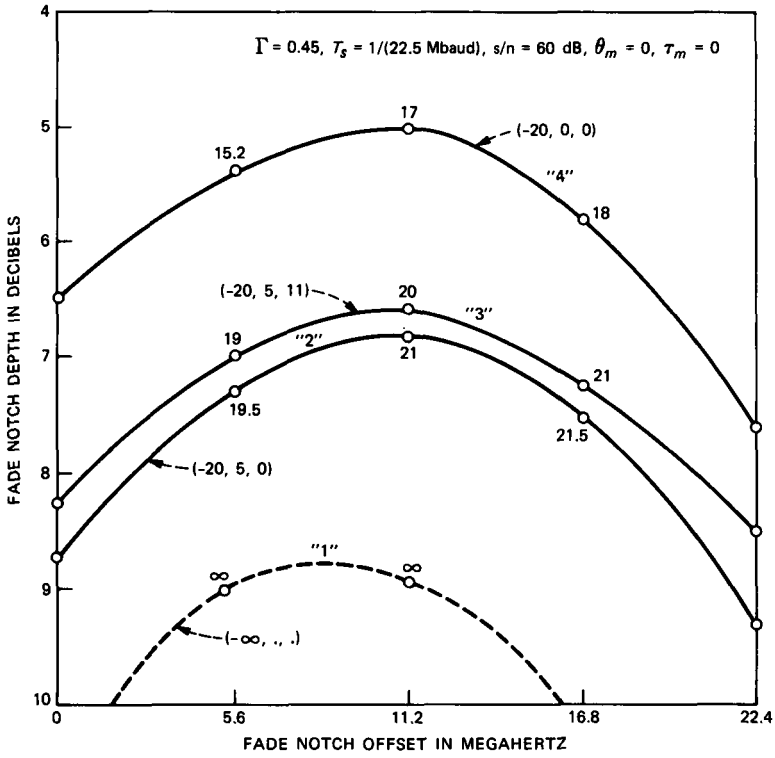


Fig. 5—Performance signature curves for dual-polarized 16-QAM radio.

signal, that is, $-20 \log |1 - \rho_I|$ versus $\Delta f_{0I}$, where $\rho_I$ is the dispersive fade notch depth of the main polarization path, and $\Delta f_{0I}$ denotes its fade notch position relative to the carrier frequency. Along the curves we have specified average signal-to-interference ratio at a selected number of points. As a reference we illustrate the signature of a single-polarized 16-QAM system, that is, $a_{II} = 0$ and label it "1." A comparison of curves labeled "2" through "4" for different fadings of the interferer in Fig. 5 reveals the aforementioned fact that the system outage time (area under the M-curve) is related to the net interfering power for a mild dispersive fading of the interfering signal on the cross-coupled path. For example, a comparison of curves 4 and 2 with the same 20-dB flat power levels and 0-MHz notch offsets reveals that curve 2 with a 5-dB inband notch fade, results in *less* outage time than the fade of curve 4 with no inband notch. Hence, the greater power loss associated with curve 2 leads to reduced outage, even though the intersymbol interference at the reference receiver in the case of curve 2 exceeds that of curve 4.

Now consider curves 2 and 3. The data corresponds to identical flat

power levels and fade notch depths, with the notch position moving from 0 MHz (notch centered) to 11 MHz (near the band edge). The notch-centered fade causes less outage than the notch offset fade because the unfaded signal spectral energy at 0 MHz is much more than that near the band edge; hence, the relationship of curves 3 and 2 is again that of diminished net signal power in the interferer resulting in a reduced outage. All these curves were computed for a 60-dB signal-to-noise ratio (s/n), 22.5-Mbaud symbol rate, $\Gamma = 0.45$ Nyquist filter roll-off, and a 16-QAM radio system.

### *2.2 Canceler model*

It is well known that interference power is directly related to the area of the cross-coupled signal power spectral density. Thus, in dual-polarized operation, where the dual-polarized signals are transmitted cochannel, any reduction of the interfering signal power spectral density area leads to a decrease in the overlap area between the main and the cross-coupled signal spectral densities, and, hence, a reduction in the interfering power. Therefore, a cross-polarized interference canceler able to perform such a task should bring about an improvement in the performance of the dual-polarized system. It is also well known that the main lobe sample of a Nyquist-type pulse is proportional to the area of its frequency spectrum. Owing to this fact, we hypothesized improvements in the dual-polarized system-performance signatures, given that the main lobe of the cross-coupled interferer is canceled in time domain. This hypothesis proved to be correct and is discussed further in Section III.

A block diagram of the cross-polarized interference canceler and system equalizers is shown in Fig. 6. Decision feedback complex taps cancel the main lobe of the cross-coupled interfering signal adaptively, using preliminary estimates of the main-lobe. Least-Mean-Square (LMS) adaptation is recommended because it was shown[7] that s/n degradation by some cross-polarization cancellation methods can be large and that the adaptive algorithm should take into account noise power minimization.[7] This is known to be one of the salient features of the LMS algorithms.[8] Because the proposed cancellation is performed at baseband, the difference between input and output of the detector slicer circuit (error signal) can be employed as the performance measure and it can be utilized by the LMS controller to derive the canceler coefficients.

Note that in Fig. 6 the baseband canceler precedes the system equalizers. This is to prevent the equalizers from causing excessive dispersion in the interfering signal when attempting to equalize deep fade notches of the copolarized signal as is the case in combined cross-polarized cancellation and ISI equalization. Note that the system

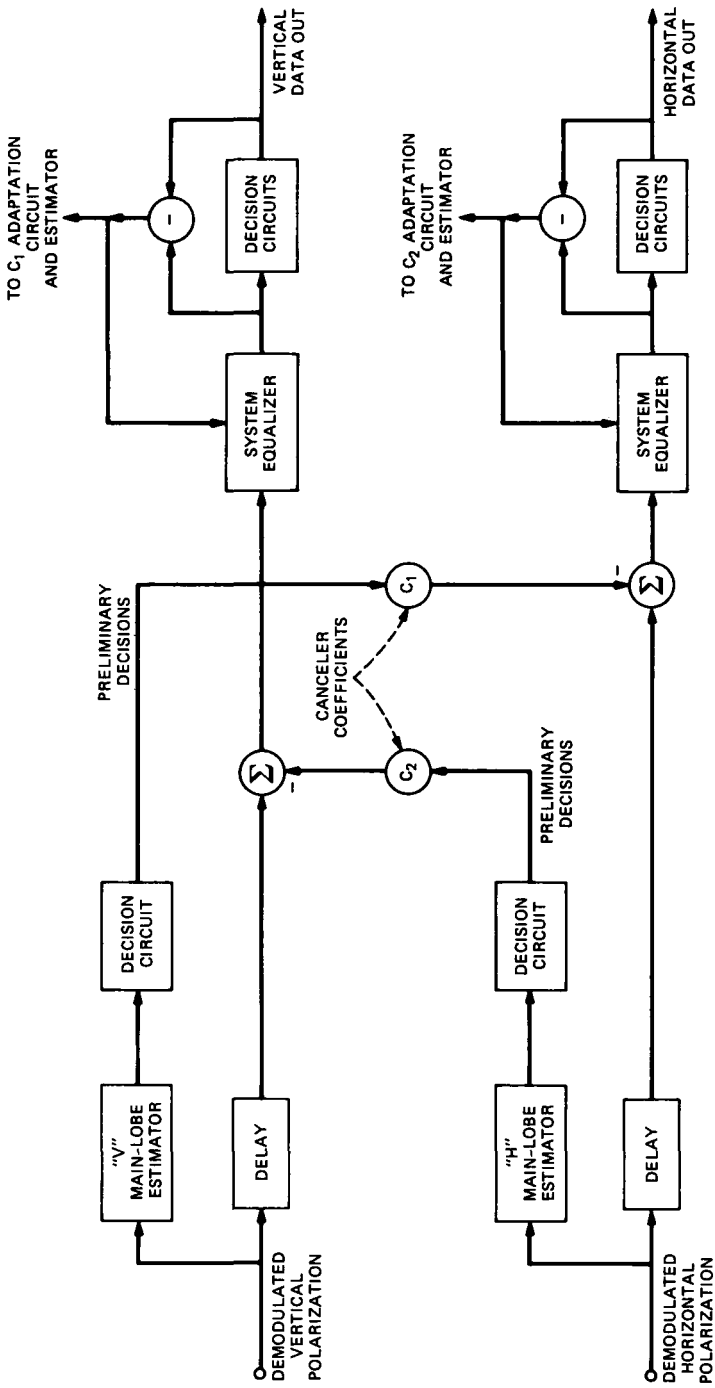


Fig. 6—Cross-polarized canceler/equalizer structure.

equalizers are used to mitigate intersymbol interference and cross-rail interference; therefore, they are not parts of the cross-polarization cancellation operation.

To perform main-lobe cancellation in practice, preliminary estimates of the signal main lobe on one polarization must be subtracted from the opposite polarization received signal that needs to be delayed by the amount of time that it takes to estimate the lobe.

In this theoretical study we assume the preliminary estimates of the signal main lobe are correct so that we can cancel the cross-polarized signal. In practice this assumption is valid in the steady-state mode of operation if some kind of bootstrapped algorithm is adopted. This, of course, adds to the circuit complexity. An obvious advantage of this method is that the preliminary decisions used to cancel the cross-polarized signal provide noise-free estimates; hence, less s/n degradation is caused by coupling mechanism compared to feedforward methods.

In the next section we elaborate on the system performance signatures after cross-polarization interference cancellation as well as making comparisons to the signatures of the same system without cross-polarization cancellation that we use as base-line measures.

## III. CANCELER PERFORMANCE

In this section we present the computed performance signature curves for dual-polarized M-QAM signals using the canceler described in the previous section.

Results in the form of performance signatures are illustrated in Figs. 7 through 10. As we can observe, use of a single complex decision feedback tap to cancel the real and imaginary parts of the cross-coupled interferer main-lobe sample renders performance signatures practically identical to those of a single-polarized system, in dual-polarized operation. To elaborate on the required number of canceler taps, it should be obvious in this case that only a single complex tap is adequate to remove the main lobe of the interferer. This is because when there is no fading or when there is offset fading of the copolarized channel, the interferer main lobe always coincides, or approximately coincides, with the desired symbol main lobe, and only one complex feedback tap is necessary to remove it. However, in the case of midband fading of the copolarized signal, as seen in Fig. 7, the timing reference of the main path impulse response is offset from the peak of the main lobe of the interfering signal. Hence, the canceler does not perform as well for midband fades as it would for offset fades of the copolarized path. This is because, for offset fades, as the copolarized path fade notch moves toward the band edge, the timing reference of the overall impulse response moves toward the origin;[5] hence, the two peaks tend

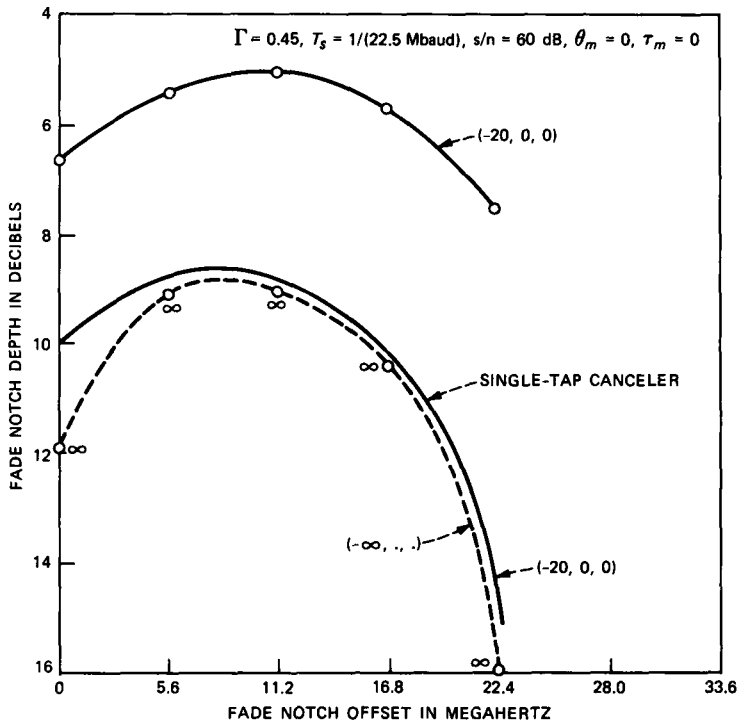


Fig. 7—Canceler performance in dual-polarized 16-QAM radio for a flat fade on cross-coupled interfering path.

to align. Of course, the remedy for the centered fade situation is to increase the number of the canceler transversal taps.

In Figs. 7 and 8, all the curves were computed for a 60-dB s/n, 22.5-Mbaud symbol rate, $\Gamma = 0.45$ roll-off, 16-QAM radio; and in Figs. 9 and 10, the signatures for 64-QAM radio were computed for a 66-dB s/n, 15-Mbaud symbol rate, and $\Gamma = 0.45$ roll-off. *Note that, in all these computations, ISI equalization of the main polarization signal is left out.*

To further quantify the influence of interfering signal main lobe on the dual-polarized system outage performance, we present an example. In the 16-QAM radio case, for an interfering signal defined by the triplet (−20, 5, 0) and for a centered fade of 6-dB notch depth on the reference copolarized signal, samples taken from $u_{i,\mathrm{I}}$, $u_{q,\mathrm{I}}$, $u_{i,\mathrm{II}}$, and $u_{q,\mathrm{II}}$ at optimum timing points are listed in Table I. As observed, the peak sample of the interferer impulse responses, $u_{i,\mathrm{II}}$ and $u_{q,\mathrm{II}}$, have amplitudes about ten times larger than the sum of absolute values of all their other samples taken every baud period. Note that, since $\theta_m$ and $\tau_m$ are zero, the imaginary part of the interferer impulse response, $u_{q,\mathrm{II}}$,

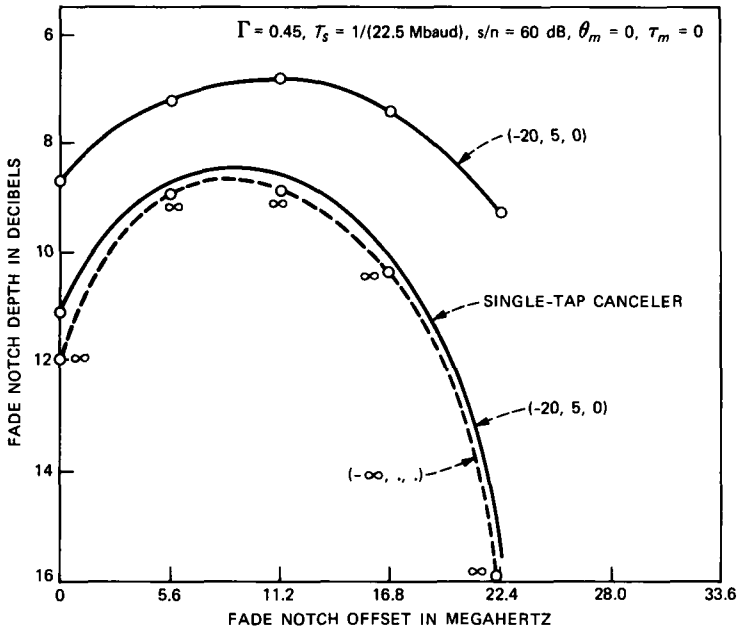


Fig. 8—Canceler performance in dual-polarized 16-QAM radio for a dispersive fade on cross-coupled interfering path.

is zero because of the notch-centered fading of the main polarization signal in this case, that is, $\phi_1 = 0$ (see Fig. 3). To ensure validity of the test, for the same interferer fading conditions, we repeated this for several different fading conditions of the copolarized signal and checked the resulting impulse responses, $u_{i,\mathrm{II}}$ and $u_{q,\mathrm{II}}$. In all the cases considered, samples of the real and imaginary parts of the interfering signal main lobe ranged somewhere between eight to ten times the value of the sum of the absolute values of all other samples. Thus, the contribution of the main-lobe sample of the interferer to the total peak distortion is much stronger than that of all other samples. Therefore, canceling the real and imaginary parts of the interferer main lobe should improve the performance significantly, as expected.

## IV. CONCLUSIONS

In this paper we proposed a novel baseband cross-polarization interference canceler structure that adaptively mitigates the interference in a dual-polarized M-QAM radio system. Employing performance signatures (M-curves) for dual-polarized systems, as introduced in Ref. 5, we showed that for synchronous transmitters, a single-decision feedback complex matrix tap canceler can enhance a dual-polarized system availability time to values close to the availability

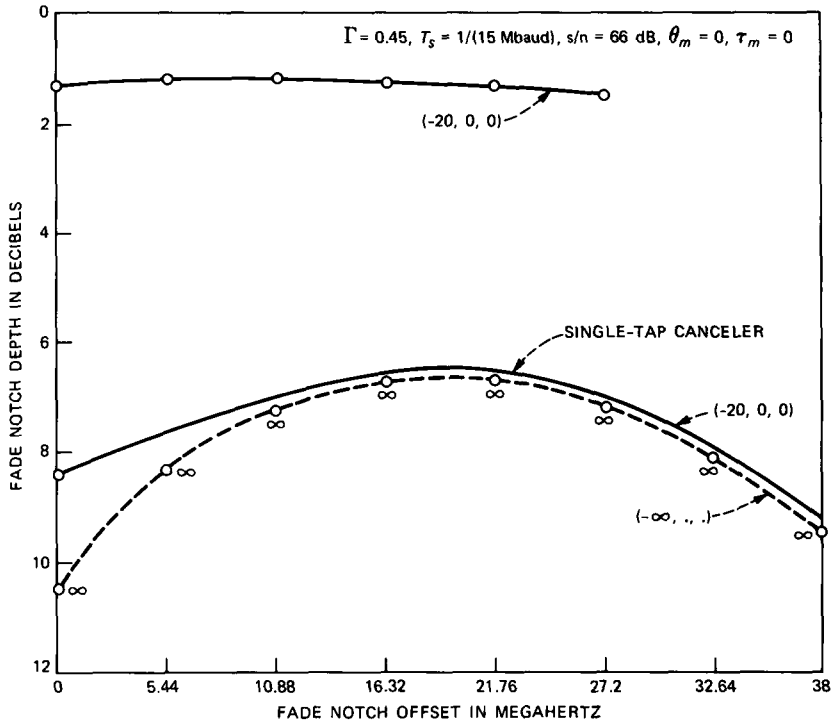


Fig. 9—Canceler performance in dual-polarized 64-QAM radio for a 20-dB flat fade on cross-coupled interfering path.

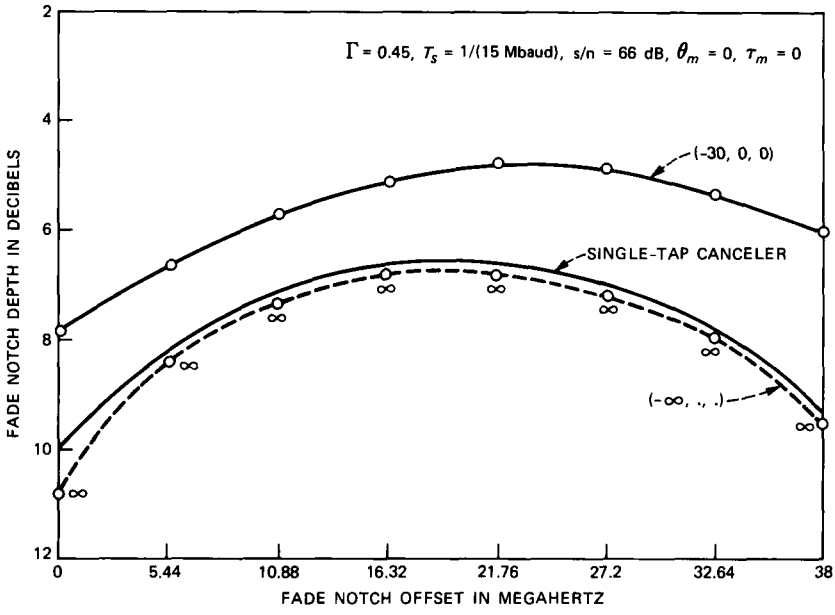


Fig. 10—Canceler performance in dual-polarized 64-QAM radio for a 30-dB flat fade on cross-coupled interfering path.

Table I—Impulse response samples of received in-phase signal on reference polarization

| $u_{i,I}$ | $u_{q,I}$ | $u_{i,II}$ | $u_{q,II}$ | Time |
|---|---|---|---|---|
| 0.5462E-04 | 0.3645E-19 | 0.7532E-05 | 0.1074E-19 | $t_0 + 9T_s$ |
| 0.1560E-04 | 0.1690E-18 | −0.7399E-06 | 0.9008E-20 | . |
| −0.1268E-03 | −0.1694E-18 | −0.1594E-04 | −0.2812E-19 | . |
| 0.3483E-04 | −0.2848E-18 | 0.1042E-04 | −0.4691E-20 | . |
| 0.3412E-03 | 0.6616E-18 | 0.3914E-04 | 0.8339E-19 | . |
| −0.3989E-03 | 0.3152E-18 | −0.6560E-04 | −0.5668E-19 | . |
| −0.1374E-02 | −0.3568E-17 | −0.1411E-03 | −0.3695E-18 | . |
| 0.7526E-02 | 0.9137E-17 | 0.9628E-03 | 0.1635E-17 | $t_0 + 2T_s$ |
| −0.2679E-01 | −0.2553E-16 | −0.3555E-02 | −0.5556E-17 | $t_0 + T_s$ |
| 0.5328E+00 | 0.1171E-14 | 0.5860E-01 | 0.1354E-15 | $t_0$ |
| −0.1332E-01 | −0.1469E-15 | 0.6797E-03 | −0.7793E-17 | $t_0 - T_s$ |
| 0.2236E-02 | 0.3376E-16 | −0.2800E-03 | 0.1649E-17 | $t_0 - 2T_s$ |
| −0.1519E-02 | −0.9138E-17 | −0.6131E-04 | −0.6031E-18 | . |
| 0.5787E-03 | 0.4275E-18 | 0.7905E-04 | 0.1154E-18 | . |
| 0.8068E-04 | 0.1226E-17 | −0.1024E-04 | −0.5979E-19 | . |
| −0.1865E-03 | −0.3837E-18 | −0.2098E-04 | −0.4639E-19 | . |
| 0.2264E-04 | −0.2996E-18 | 0.8858E-05 | −0.7337E-20 | . |
| 0.7182E-04 | 0.2201E-18 | 0.6764E-05 | 0.2058E-19 | . |
| −0.2951E-04 | 0.7752E-19 | −0.5842E-05 | −0.2163E-20 | $t_0 - 9T_s$ |

time for a single-polarized radio system, for the assumed propagation model.

## REFERENCES


1. C. A. Baird and G. Pelchat, "Cross Polarization Techniques Investigation," Harris Corporation Report No. RADC-TR-77-244, July 1977.
2. B. E. Gillingham et al., "Cross Polarization Interference Reduction Techniques," Harris Corporation Report No. RADC-TR-79-154, June 1979.
3. J. Namiki and S. Takahara, "Adaptive Receiver for Cross-Polarized Digital Transmission," Int. Conf. Commun., June 14–18, 1981, Denver, Colorado, Paper 46.3.1.
4. M. L. Steinberger, "Design of a Terrestrial Cross-Pol Canceler," Int. Conf. Commun., June 1982, Philadelphia, pp. 2B.6.1–5.
5. M. Kavehrad and C. A. Siller, private communication.
6. W. D. Rummler, "A New Selective Fading Model: Application to Propagation Data," B.S.T.J., *58*, No. 5 (May–June 1979), pp. 1037–71.
7. M. Kavehrad, "Performance of Cross-Polarized M-ary QAM Signals Over Nondispersive Fading Channels," AT&T Bell Lab. Tech. J., *63* (March 1984), pp. 499–521.
8. J. G. Proakis, *Digital Communications*, New York: McGraw-Hill, 1983.


## AUTHOR


**Mohsen Kavehrad,** B.S. (Electrical Engineering), 1973, Tehran Polytechnic Institute; M.S. (Electrical Engineering), 1975, Worcester Polytechnic Institute; Ph.D. (Electrical Engineering), 1977, Polytechnic Institute of New York; Fairchild Industries, 1977–1978; GTE, 1978–1981; on the faculty of Northeastern University, 1981–1984; AT&T Bell Laboratories, 1981—. At AT&T Bell Laboratories Mr. Kavehrad is a member of the Communications Methods Research Department. His research interests are digital communications and computer networks. He is a Technical Editor for the IEEE Communications Magazine. He established and was the Chairman of the IEEE Communications Chapter of New Hampshire in 1984. Member, IEEE, Sigma Xi.